

WAVE-CURRENT INTERACTIONS IN MARINE CURRENT TURBINES

N. Barltrop¹, A. Grant², K. S. Varyani¹, D. Clelland¹, X. P. Pham¹

Abstract

The influence of waves on the dynamic properties of bending moments at the root of blades of tidal stream vertical axis rotors is reported. Blade theory for wind turbine is combined with linear wave theory and used to analyse this influence. Experiments were carried out to validate the simulation and the comparison shows the usefulness of the theory in predicting the bending moments. The mathematical model is then used to study the importance of waves for the fatigue design of the blade-hub connection.

KEYWORDS: Tidal stream, current turbine, wave-current interaction, linear blade theory.

1. Introduction

Horizontal-axis wind turbines have achieved a dominant position in the market, and for tidal streams, the arguments in their favour are even more compelling [2,7,8,10]. Reversing gravity loads, which are very important for horizontal-axis wind turbines, should be much less important because buoyancy can be used to balance the blade weight. Deterministic cyclic loading (from velocity shear and yaw error effects) may be important. For horizontal-axis machines in a tidal stream relatively low levels of turbulence minimise the stochastic structural loads, that can be very important for wind turbines, but the effect of waves is likely to be important.

It is desirable to locate rotors near the free surface to make maximum use of the available cross-sectional area and to intercept the highest stream velocities. The effect of waves may therefore be important in determining limits for device location and rotor operational envelopes. A substantial body of knowledge on wave loading already existed, but not in this context. There was an urgent need for research to determine the response and practical limitations posed by the associated phenomena.

The main objectives of this study were to both assess our mathematical modelling capability and to consider limits imposed by waves on the performance of tidal stream rotors. In this paper, the authors look into fatigue from bending moments acting about the roots of tidal stream rotors. Experiments are carried out and data are used to validate simulation results based on a mathematical model, i.e. linear wave and blade element theory. The model is then used to assess the significance of wave induced fatigue on the design of the blade root-rotor hub connection. Related papers overlap with this one in describing the experiments and theory of the numerical model but consider blade bending behaviour in more detail[11] and the effect of waves on power output[12].

2. Theory

The torque, thrust and bending moments induced by the flow are calculated based on linear blade theory as in [1]. Each blade of the wind turbine is divided into a number of sections (Fig.1). Chord and pitch or twist angle vary are taken as constant in each section. Lift and drag coefficients, as functions of incidence angles are then calculated and (optionally) adjusted appropriately to account for 3-d delayed stall effects. Velocities of water flow passing the blade section are next calculated taking into consideration the effects from current and waves. Current changes the encountered wave frequency:

$$f_e = \frac{1}{T_e} = \frac{1}{T_w} + \frac{U_c}{L_w} \cos(\theta_w)$$

where U_c is the current velocity, T and L are wave period and length, respectively. Subscript 'e' and 'w' represent encountered and wave relative to the current, respectively. θ_w is the incident angle of current.

¹ Department of Naval Architecture and Marine Engineering, Universities of Glasgow and Strathclyde, Scotland, UK.

² Department of Mechanical Engineering, University of Strathclyde, Scotland, UK.

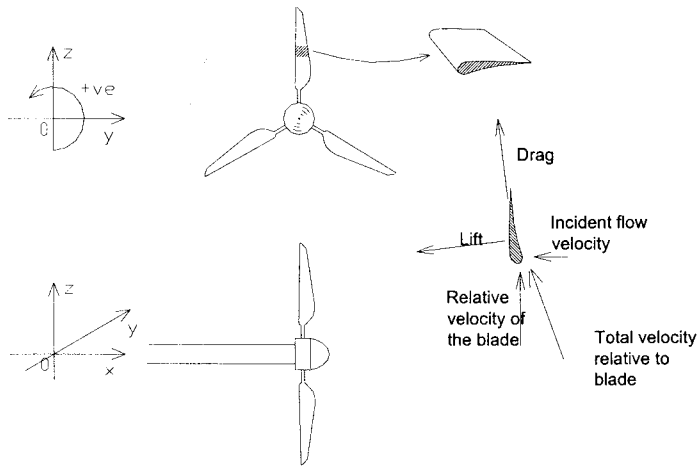


Figure 1: Co-ordinate system and velocity diagram in blade theory.

Wave kinematics are calculated using linear wave theory:

Horizontal wave particle velocity:

$$u = \frac{\pi H}{T_w} \frac{\cosh[k_w((zr - ds) + d)]}{\sinh(k_w d)} \cos(\phi_w)$$

H = wave height

T_w = wave period

k_w = wave number

d = water depth

ds = rotor axis depth

zr = instantaneous vertical position of centroid of blade section with respect to rotor axis

ϕ_w = angle of attack

Vertical wave particle velocity:

$$v = \frac{\pi H}{T_w} \frac{\sinh[k_w((zr - ds) + d)]}{\cosh(k_w d)} \sin(\phi_w)$$

The interaction of the flow with the turbine is calculated using blade element – momentum theory. This was implemented by modifying an existing program to add in the extra wave particle velocities. The normal to rotor plane horizontal velocity and the vertical wave particle velocities were simply added to the incident current velocity. (Fig. 1). Note that tip loss from the blade is also introduced into the equations. The tip loss coefficient F is a function of distance r from the blade tip and the distance s between the vortex sheets assumed to emanate from the rotor:

$$F(\phi, r) = \frac{2}{\pi} a \cos \left[\exp \left[-\pi \frac{(R - r)}{s} \right] \right]$$

The distance s was calculated in a number of different ways and the method can have a large influence on the results. Simply using the incident flow velocity without allowing for the effect of the induction factor a seemed to work reasonably well and avoided problems when a changed considerably through the cycle.

The torque acting on the rotor is then the sum of torques acting on individual blades which in turn is the sum of products of the in-plane components of the lift and drag forces and the arm lengths from centres of blade sections to root of blade. Thrust on the rotor, similarly is the sum of out-of-plane components of lift and drag force on all the blade sections of all the blades on the rotor.

In and out of plane bending moments acting at the root of each blade are calculated in the similar fashion, but use the results for each blade separately.

The calculations are carried out time step by time step assuming steady flow conditions at each step.

삭제됨:

3. Rotor design and manufacture

For the project, three rotor designs were produced, with progressive refinement based on results of testing. The largest practical rotor diameter was used to minimise scale effects. This paper concentrates on the first rotor [4], which was essentially a wind turbine configuration, with a slight increase in blade chord and thickness for structural strength. The aerofoil profile (NREL S814) was chosen for its good performance at low Reynolds numbers, and its tolerance of surface imperfections. The rotor has three blades, and an overall diameter of 350 mm. At the root, the blades taper down to a circular section, to facilitate the fitting of strain gauges.

The S814 is one of the series developed by NREL, USA for wind turbines. One particularly important characteristic of the S814 is the minimal sensitivity of its maximum lift coefficient to roughness effects, a critical property for stall-regulated wind turbines. The aerofoil has a very low drag coefficient and is also not sensitive to change of angle of attack at around stalling angle. The profile shape is illustrated in Figure 2a; specific technical features of the NREL S814 are detailed in [9]. The length of the blade used for rotor 1 was 150 mm with maximum chord of 44 mm. Nominal chord length at the tip was 20 mm, but the tip was rounded to reduce shed vortices. Chord and pitch distributions are shown in Figure 2b; an increase of about 5° from the nominal pitch angle was found to give best performance.

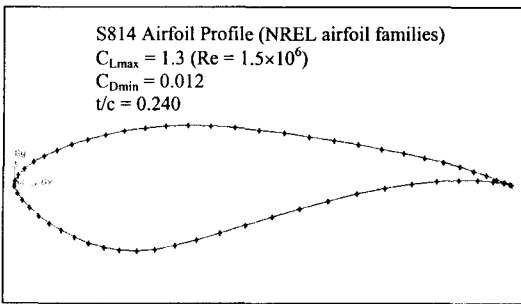


Figure 2a: Sectional profile of NREL S814 blade.

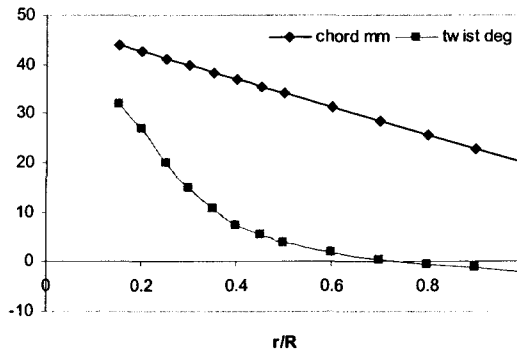


Figure 2b: Chord and pitch distribution along blade.

Figure 2c shows the 2D characteristics of lift and drag coefficients based on tunnel tests at Reynolds number of 3×10^6 .

4. Experiment

Rotor performance (shaft torque, axial thrust and blade bending moments) was investigated in the Universities of Glasgow and Strathclyde 77 x 4.6 x 2.4m deep wave/towing tank. A two dimensional aerofoil section 'boat' made of glass fibre (Figure 3a) was used to house the motor, gearing and torque and thrust transducers. The rotor was supported in front of the boat which itself was cantilevered down from the towing tank carriage as shown in Figures 3b and 3c.

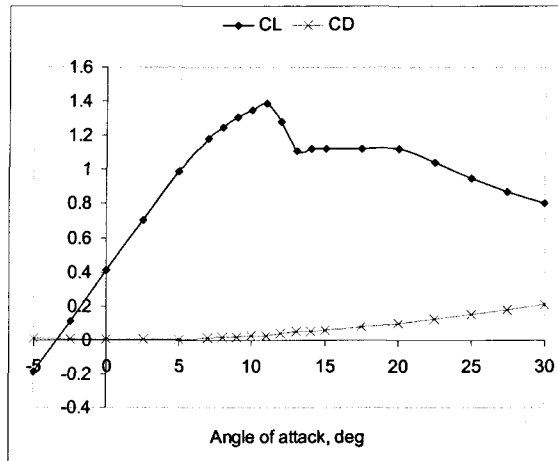


Figure 2c: Lift and drag coefficients based on tunnel tests at $Re = 3 \times 10^6$.

Strain gauges were used for the measurement of bending moments about the root of the blade in the case of rotor I. The strain gauges were made water tight using M-Line J-Coat. The shaft to which the rotor is attached was hollow. The cables of the strain gauges were accommodated through the inside of the shaft and the signals were transferred through slip rings. Provision was made for amplifying the signals before passing them through the sliprings but slipring tests and the final results demonstrated good performance without the need for amplifiers on the rotating shaft. The shaft was supported by linear bearings to allow rotation and axial movement. To allow precise

speed control a motor/generator with gearbox and tachometer was used with closed loop control. The motor/generator could provide power (at low current speeds) or absorb power (at the higher current speeds). The shaft extended in front of the boat bow sufficiently for minimal interference between the boat and the rotor. A grease box prevented the entry of water around the shaft. The boat was clamped and bolted by steel beams to a rail mounted moving carriage over the tank. The carriage moved the boat along the tank at steady speed to simulate tidal currents. A flap type wave generator produced waves of a known wavelength and period. These are of course encountered at a higher frequency than the generated wave frequency when the rotor is moving towards the waves. (Note that, within the limitations of potential flow theory the model was a precise Froude scaled representation of the real case of a fixed rotor encountering waves of the generated length on the current). It should however be noted that in these tests, the Reynolds number varies in the range of 4.32×10^3 to 6.0×10^4 which is significantly lower than the range of 0.75×10^6 to 1.5×10^6 for S814 data. Low Reynolds number can degrade the dynamical properties of the airfoil and can be potential source of discrepancy between the test data and the simulation data.

Experiments were carried out to test the performance of the tidal stream rotors for different conditions. The most important parameters were the dynamic properties of the rotor under different wave-heights, wave frequencies and current speeds. Only the first rotor was strain gauged because the requirements for high stresses in the root under the towing test conditions were not compatible with the need to load the rotor more highly to obtain a high Reynolds number in cavitation tests. The experiments covered a range of towing speeds (0.0 – 1.6 m/s), wave heights and frequencies, and depths of immersion whilst the rotational speed was set at about 200rpm. The aims were to investigate the magnitude and variation of thrust, torque and bending moment at the root of the blade. The results were then compared with calculations. For tests at low velocities, the starting position of the testing is set at approximately one third of the tank length from the beach so that reflected waves from the beach would not reach the turbine by the end of the test run. It should be noted that the tests are not scale models of a realistic situation, the full scale rotor rpm and the incident velocity are much higher than might realistically be expected. The higher velocities were used to obtain larger forces and bending moments which were better for validating the theoretical model. To demonstrate the validity and some limitations of the simple model, this paper presents the bending moments acting about the roots of blades of rotor 1 in waves of 150 mm height (model scale) and two frequencies, i.e. 0.5 Hz and 1.0 Hz

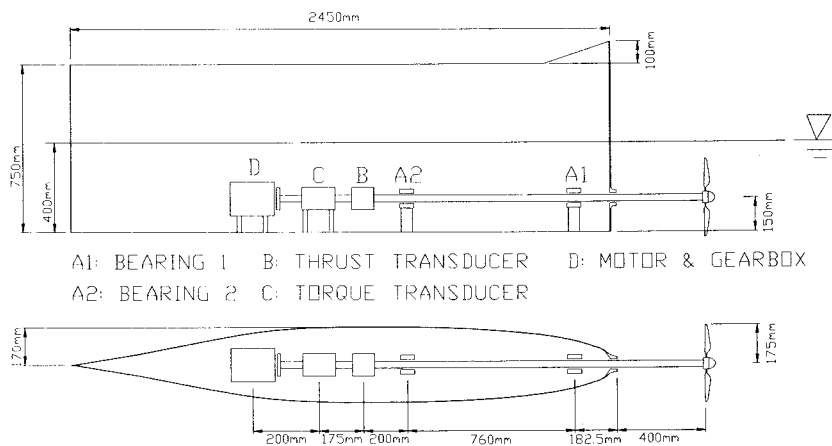


Figure 3a: Arrangement of rotor and devices.

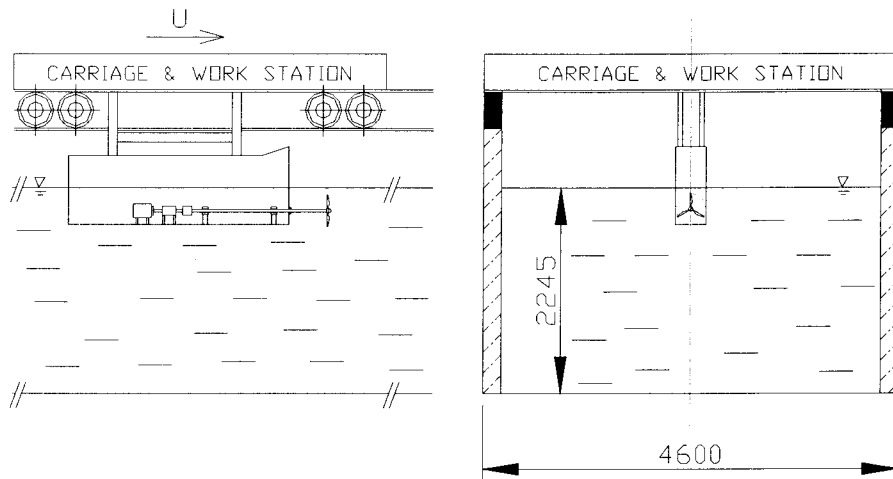


Figure 3b: Profile and cross-section views of the experiments.

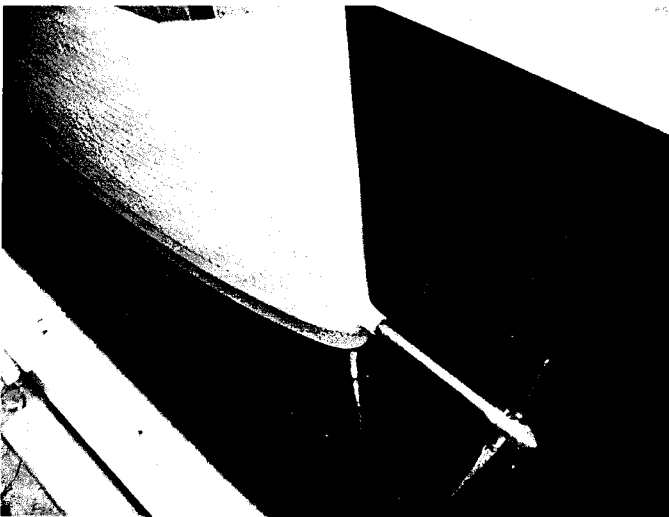


Figure 3c: Model being lowered into the tank

5. Validation

5.1 Long waves of 150 mm height and 0.5 Hz frequency

Figures 4a,b and 4c,d show dynamic properties of bending moments about roots of rotor blades in waves of 0.5Hz frequency and 150mm height at current speeds of 0.3m/s and 1.0m/s (at model scale), respectively. The wave steepness is low: 1/40. The corresponding tip-speed-ratios, based on the mean velocity, are 12.22 and 3.77, respectively. Sim_Mx

and Sim_My represent the simulation results of out-of-plane and in-plane bending moments, respectively whilst Exp_Mx and Exp_My refer to their corresponding experimental results. As can be seen, in long waves, blade element with linear wave theory can predict the dynamic response of both out-of-plane and in-plane bending moments.

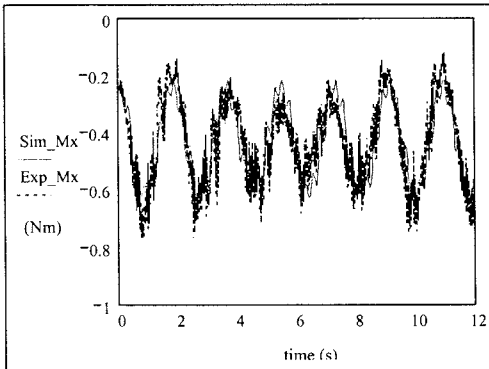


Figure 4a: Out of-plane bending moment in waves of 150 mm height and 0.5 Hz frequency and current speed of 0.3 m/s at model scale.

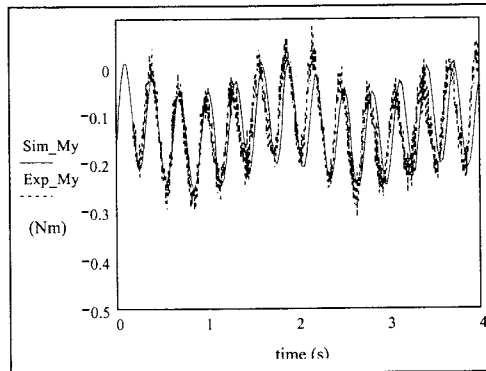


Figure 4b: In-plane bending moment in waves of 150 mm height and 0.5 Hz frequency and current speed of 0.3 m/s at model scale.

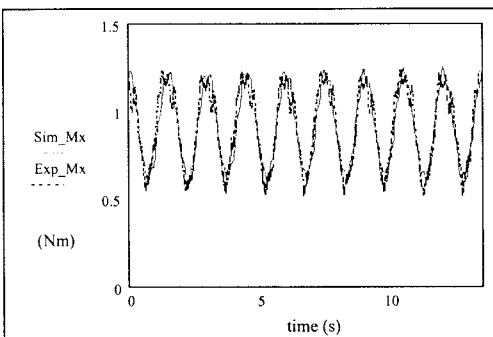


Figure 4c: Out of-plane bending moment in waves of 150 mm height and 0.5 Hz frequency and current speed of 1.0 m/s at model scale.

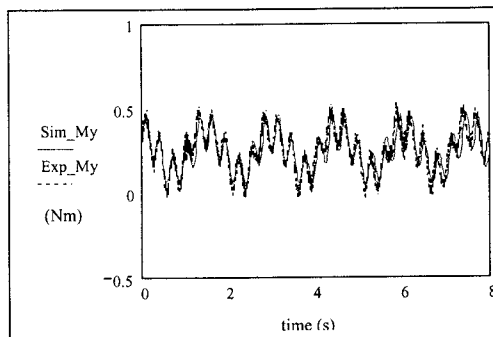


Figure 4d: In-plane bending moment in waves of 150 mm height and 0.5 Hz frequency and current speed of 1.0 m/s at model scale.

5.2. Steep waves of 150 mm height and 1.0 Hz frequency

Figures 5a,b and 5c,d show the dynamic properties of bending moments about roots of rotor blades in steep waves of 1.0Hz frequency and 150mm height at current speeds of 0.3m/s and 1.0m/s, respectively. The corresponding tip-speed-ratios are again 12.22 and 3.77, respectively. The wave steepness is 1/10. It can be seen that blade element with linear wave theory can predict relatively well the fluctuation of in-plane bending moment (My) both in low and high current speed ranges. However, for out-of-plane bending moment, the fluctuation predicted is less than that measured. Figures 4a and 4c show that the amplitude of bending moment variation recorded during the test is of order of two times that predicted. This highlights the significance of high non-linearities associated with steep waves but it also seems likely that the tip loss factor is having a large effect on these analysis results, since using a different equation can considerably improve the results..

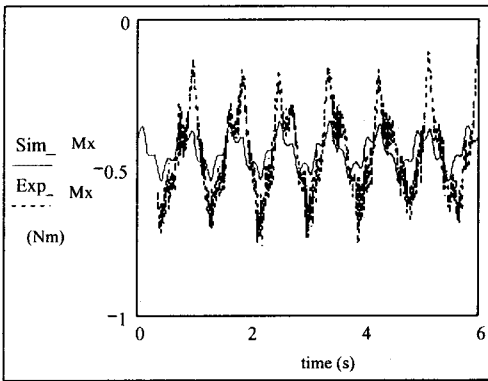


Figure 5a: Out of-plane bending moment in waves of 150 mm height and 1.0 Hz frequency and current speed of 0.3 m/s at model scale.

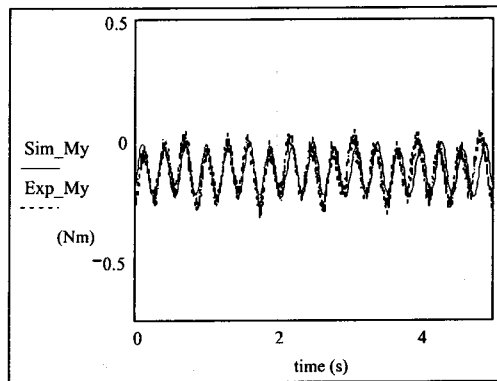


Figure 5b: In plane bending moment in waves of 150 mm height and 1.0 Hz frequency and current speed of 0.3 m/s at model scale.

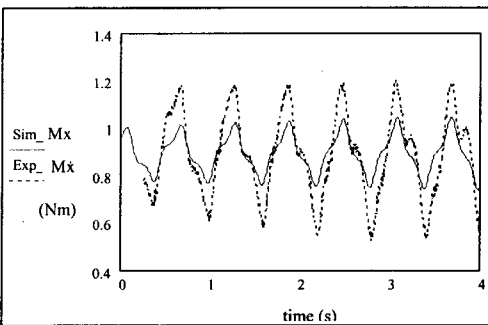


Figure 5c: Out-of-plane bending moment in waves of 150 mm height and 1.0 Hz frequency and current speed of 1.0 m/s at model scale.

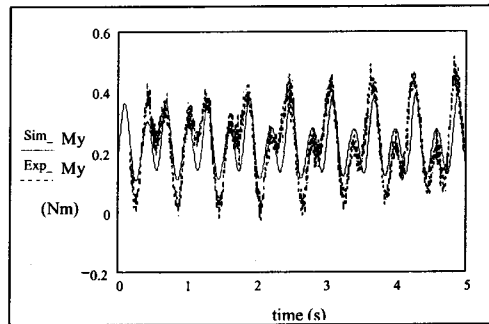


Figure 5d: In plane bending moment in waves of 150 mm height and 1.0 Hz frequency and current speed of 1.0 m/s at model scale.

5.3 General discussion

A general observation on the dynamic characteristics of bending moments at the root of a rotor blade is that it sees the main oscillation at the encountered wave frequency. The rotor frequency shows in the smaller superimposed oscillation in the in-plane bending moment and is mainly the self-weight effect. The numerical model is clearly giving reasonable results in less steep waves, especially in the middle of the short segment of time history where the numerical wave has been synchronised with the measured wave (Figure 5b). (It is interesting that in the steep waves the difference between the linear wavelength and the non-linear wavelength results in a loss of synchronisation between rotor position and wave phase in just a few wave cycles. This is significant when comparing predictions with measurements but is not important for design.)

6. Case study using linear blade simulation model

A case study was performed for a 20m 2 bladed diameter turbine, in 28m of water with the rotor axis at 14m depth. The machine was assumed to operate at variable speed but to have a tip speed ratio, relative to the current, of 2π . The blade characteristics were as described above.

The wave and current climates were based on *factored* Southern North Sea measurements (basic data had an annual wave height of 11m, max tidal current about 1m/sec). However it was assumed that turbines are likely to be placed in estuary locations where currents are magnified but wave height will have been dissipated by bottom friction, so the current speeds were increased and the wave heights reduced.

The waves occurrences were taken to be defined by a log-linear probability of exceedence - wave height relationship.

$$n(h > H) = 10^{\log(N1) \left(1 - \frac{H}{H1}\right)}$$

where n is the number of waves exceeding height H
 $N1$ is the number of waves per year (approx 6×10^6)
 $H1$ is the height of wave exceeded on average once per year.

Analyses were performed with $H1 = 3, 6$ and $9m$.

The current occurrences were based on measurements and had a maximum tidal component of $1m/sec$. Including wind and surge effects the current exceeded once per year is $1.75m/sec$. The current exceedence distribution is shown in Figure 6b. This distribution was factored up so that the maximum tidal component became $1, 2$ or $3m/sec$.

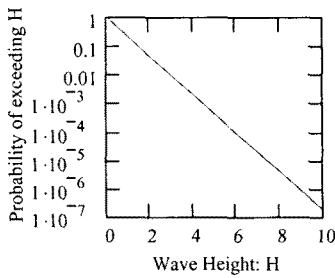


Figure 6a: Unfactored wave height distribution

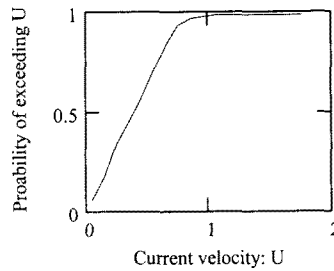


Figure 6b: Unfactored current velocity distribution

It was assumed that there was no correlation between current and waves.

The turbine model was run for an array of regular waves and currents and the time histories of the in and out of plane blade root bending moments found. (Regular waves were used, this can give misleading results owing to the deterministic phase relationship between the rotor and waves. However the results showed sensible trends.) In the calculations the assumption was made that the waves and currents were always running in the same direction. This is not a requirement of the software but reduced the number of simulations required.

The probability of each wave and current combination was calculated as the product of the independent probabilities of the wave and current being in the range represented by each combination. Note that at this stage the different maximum wave heights and currents were selected in defining the probability distributions that were used.

The moment time histories were rainflow counted to give moment range values that can be used in a fatigue analysis.

The moment ranges were then converted to stresses using an assumed $0.6m$ diameter by $60mm$ thickness blade root.

S-N curve were selected. Welded steel hubs have been found to have inadequate fatigue life for wind turbines and it is quickly apparent that they would also be inadequate for a tidal stream turbine subject to significant wave action. So S-N curves and stress concentration factors corresponding to a cast iron hub:

S-N curve stress at 10^7 cycles = $140MPa$, slope = 20 , scf = 0.5

or non welded steel connecting components at the blade root:

S-N curve stress at 10^7 cycles = $100MPa$, slope = 4 below 10^7 cycles and slope = 6 above 10^7 cycles, scf = 2

were selected. See Figure 6c.

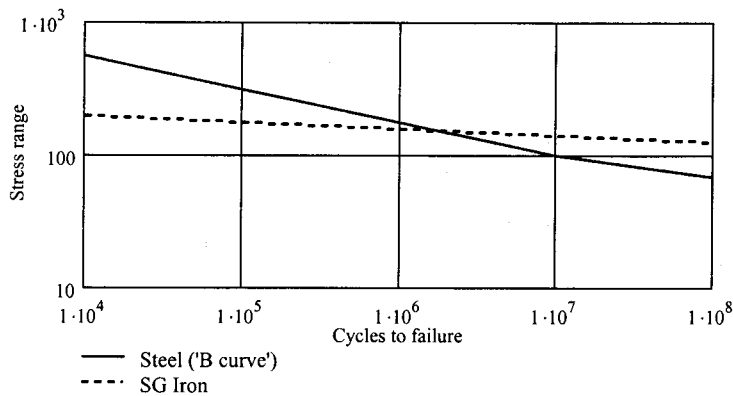


Figure 6c: S-N curves used in the analysis

The different stress concentration factors (scfs) take into account the opportunity to provide substantial thickness in a casting which can reduce stresses to below the nominal level and the tendency for steel components to have threads or other stress concentrations that tend to increase stresses to greater than the nominal values. Often steel components have a lower area than the blade root but are used in prestressed connections, this has the effect of making the blade root assist in the transfer of dynamic loads, so reducing fatiguing stress ranges. Cast iron fatigue varies considerable according to the type of cast iron material. Immersion in sea water also affects the fatigue behaviour, reducing fatigue life generally and especially in the high cycle region. Clearly the values selected for both materials are only indicative, the actual values that should be used for any given turbine need to be assessed taking into account the geometry and materials used.

Using, for each rainflow counted stress time history, the probability (selected according to the specified maximum wave height and maximum current) and the S-N curve and scf the total annual damage and estimated fatigue lives were calculated.

The results for the steel case are shown in Table 6a.

		Maximum tidal current		
		1m/s	2m/s	3m/s
Annual Maximum	3m	775	542	50
	6m	98	39	4
Wave Height	9m	15	5	1

Table 6a: Fatigue lives for the tidal current and annual wave height combinations

The results for the cast iron show a much greater variation as a result of the shallower S-N curve slope.

Sensitivities were also run to consider the effect of different operating strategies, particularly shutting down the turbine when wave heights exceeded a specified value. This was found to be beneficial for the cast iron components but not so beneficial for the steel. This is a result of cast iron's shallow S-N curve, which implies that cast iron is more sensitive to damage by small numbers of high stresses cycles than steel.

This is shown in Figure 6d.

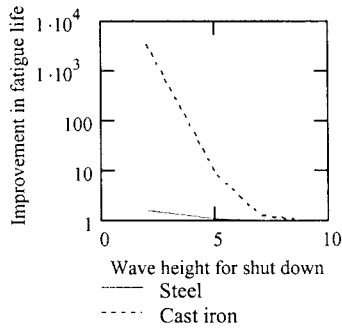


Figure 6c: Fatigue life improvement obtained by shutting down in high waves
(Note these calculations are based on regular waves, not sea states)

7. Conclusion

The paper has briefly introduced a linear blade element - momentum theory which includes wave effects in analysing dynamic properties of bending moments acting at roots of rotor blades of a tidal stream rotor. Experiments were also described in the validation of simulation results. A study of the effect of waves on the fatigue life of the blade root-hub connection suggests:

- Waves are likely to have a significant effect on the fatigue life of the blade root and hub.
- The turbine control required to avoid excessive fatigue damage depends on the material fatigue characteristics.
 - Materials with relatively high S-N curve slopes (e.g. steel with slope 3 – 6) are not too sensitive to occasional large stresses and so can keep operating in occasional higher sea states.
 - Materials with shallow S-N curves (e.g. cast iron with slope around 20) benefit from the good high cycle performance of the material but can be more sensitive to occasional large stresses from high waves.

References

1. **Eggleston, D.M. and Stoddard, F.S.** Wind turbine engineering design. New York: Van Nostrand Reinhold, 1978.
2. **Pham X., Liu Y, Varyani K., and Barltrop N.** Report on tidal stream rotor tests. Universities of Glasgow and Strathclyde, 2004.
3. **Wang D., Atlar M. and Paterson I.** Stream rotor simulation tests using marine propeller model STO192. *Report No. MT-2003-015*, School of Marine Science and Technology, University of Newcastle upon Tyne, July, 2003.
4. **Wang D., Atlar M. and Paterson I.** Performance tests of the first tidal stream rotor. *Report No. MT-2003-016*, School of Marine Science and Technology, University of Newcastle upon Tyne, October, 2003.
5. **Wang D., Atlar M. and Paterson I.** Performance tests of the second tidal stream rotor. *Report No. MT-2004-027* School of Marine Science and Technology, University of Newcastle upon Tyne, December, 2004.
6. **Wang D., Atlar M. and Paterson I.** Performance tests of the third tidal stream rotor. *Report No. MT-2005-002*, School of Marine Science and Technology, University of Newcastle upon Tyne, January, 2005.
7. Marine Current Turbines press release, 18th March 2004.
8. **Myers L. and Bahaj A. S.** Basic operational parameters of a horizontal axis marine current turbine. *Proc 8th World Renewable Energy Congress*, Denver, USA. 2004.
9. **Tangler J.L., and Somers, D.N.** NREL airfoil families for HAWTs. <http://wind.nrel.gov/>, 1995.
10. **Takamatsu, Y., Furukawa, A., Okuma, K., and Takemouchi, K.** Studies on cavitation occurring on the runner blade of a Darrieus-type cross-flow water turbines. *JSME Intl Journal, SERII, Vol. 35, No.1.*
11. **Barltrop A., GrantA., Varyani KS., Clelland D., Pham XP.,** Wave-current interactions in marine current turbines. Accepted for publication by JEME.
12. **Barltrop A., GrantA., Varyani KS., Clelland D., Pham XP.,** Investigation into Wave-Current Interactions in Marine Current Turbines. (Report of work based on rotor 2 tests). Accepted for publication by JPE.